Jones-matrix mapping of polycrystalline networks of layers of main types of amino acids

Mishalov, Volodymyr, Syvokorovskaya, Anastasia-Vira, Bachinskiy, Viktor, Sarkisova, Yuliya Yu., Ushenko, Alexander, et al.

Volodymyr D. Mishalov, Anastasia-Vira S. Syvokorovskaya, Viktor T. Bachinskiy, Yuliya Yu. Sarkisova, Alexander G. Ushenko, Olexander V. Dubolazov, Vladimir A. Ushenko, Artem V. Motrich, Mashat Kalimoldayev, Waldemar Wójcik, Andrzej Smolarz, Zhazira Amirgaliyeva, "Jones-matrix mapping of polycrystalline networks of layers of main types of amino acids," Proc. SPIE 11456, Optical Fibers and Their Applications 2020, 1145606 (12 June 2020); doi: 10.1117/12.2569783

SPIE.

Event: Optical Fibers and Their Applications 2020, 2020, Bialowieza, Poland

Jones-matrix mapping of polycrystalline networks of layers of main types of amino acids

Volodymyr D. Mishalov*[a], Anastasia-Vira S. Syvokorovskaya[b], Viktor.T. Bachinsky[b], Yuliya, Yu. Sarkisova[b], Alexander G. Ushenko[c], Olexander V. Dubolazov[c], Vladimir A. Ushenko[c], Artem V. Motrich[c], Mashat Kalimoldayev[d], Waldemar Wójcik[e], Andrzej Smolarz[e], Zhazira Amirgaliyeva[d,f]
[a]Shupik National Medical Academy of Postgraduate Education, 9 Dorohozhytska St., Kyiv, Ukraine 04112; [b]Bukovinian State Medical University, Teatral'na Square 2, Chernivtsi, Ukraine 58000; [c]Yuriy Fedkovych Chernivtsi National University, 2 Kotsyubyns'koho St, Ukraine 58012; [d]Institute of Information and Computational Technologies CS MES RK, Almaty, Kazakhstan; [e]Lublin University of Technology, Lublin, Poland; [f]Al-Farabi Kazakh National University, Kazakhstan

ABSTRACT

The given data on the optical arrangement, in which the coordinate distributions of the real and imaginary component of the elements of the Jones matrix of optically thin polycrystalline layers are determined. Algorithms are presented and an experimental method for measuring the real and imaginary component of Jones-matrix images is analyzed. The experimental results of the study of statistical, correlation, and fractal parameters, which characterize the real component of the Jones-matrix image of polycrystalline networks of flat layers of the main types of human amino acids, are presented.

Keywords: polarization, interference, anisotropy, cartography

1. INTRODUCTION

The actual direction in laser polarimetric diagnostics[1,2,3] of biological objects is the development of matrix methods[4,5,6], which provide the most complete information about the polycrystalline structure[7,8,9] of films of biological fluids[10, 11, 12] of human organs of different morphological structure and physiological state[13,14,15].

Our work is devoted to the development and experimental testing of the Johns-matrix mapping method for polycrystalline layers of basic amino acids of the human body in order to obtain objective criteria for the differential diagnosis of pathological conditions.

2. OPTICAL SCHEME OF JONES-MATRIX MAPPING OF FILMS OF OPTICAL-ANISOTROPIC BIOLOGICAL FLUIDS

Figure 1 shows the optical scheme of a polarimeter for measuring the totality of the coordinate distributions of the real and imaginary components of the Jones matrix of biological fluids. The illumination was carried out in parallel ($\varnothing$ = 104μm) by a He-Ne laser beam (λ = 0.6328μm, W = 5.0mW). The polarization illuminator consists of quarter-wave plates 3; 5 and polarizer 4, which ensures the formation of a laser beam with an arbitrary azimuth or polarization ellipticity $0° \le \beta_0 \le 90°$

Polarization images of films of biological fluids were projected by micro-lens 7 (4× magnification) on to the photosensitive area (800×600 pixels) of a CCD camera 10, which provided a measuring range of structural image elements for the following sizes 2-2000μm. The experimental conditions were selected so as to virtually eliminate the spatial-angular aperture filtration when imaging films of biological tissues. This was ensured by matching the angular characteristics of the light scattering indicatrices with samples of films of biological fluids $\Omega \approx 16°$ and the angular aperture of the micro-lens ($\Delta\omega = 90°$). Here Ω is the angular cone of indicatrices, in which 98% of the total energy of the scattered radiation is concentrated. Image analysis of films of biological fluids was carried out using a polarizer 9 and a quarter-wave plate 8.

*e-mail: inter-dep@nmapo.edu.ua

Optical Fibers and Their Applications 2020, edited by Ryszard S. Romaniuk, Jan Dorosz, Proc. of SPIE Vol. 11456, 1145606 · © 2020 SPIE
CCC code: 0277-786X/20/$21 · doi: 10.1117/12.2569783

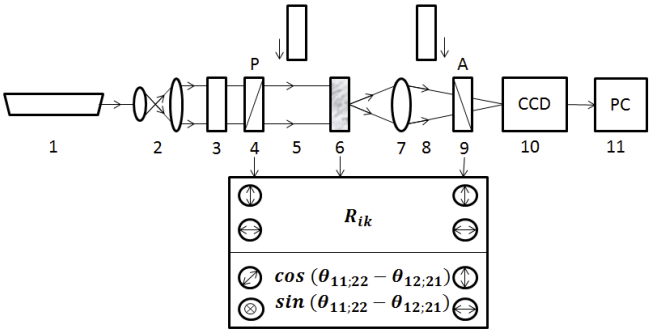

Figure. 1. The optical scheme of the polarimeter, where 1 - He-Ne laser; 2 - collimator; 3 - stationary quarter-wave plate; 5, 8 - mechanical movable quarter-wave plates; 4, 9 - polarizer and analyzer, respectively; 6 - the object of study; (b) 7 - micro lens; 10 - CCD camera; 11 - personal computer

3. JONES-MATRIX IMAGES OF POLYCRYSTALLINE NETWORKS OF OPTICALLY THIN LAYERS OF AMINO ACIDS

In order to obtain the objective criteria for the polarization manifestations of the optical anisotropy of polycrystalline networks of various types, we carried out a comprehensive study of the real component of the coordinate distributions of the elements of the Jones matrix $R_{11}(m \times n)$ and $R_{12;21}(m \times n)$, characterizing mainly the manifestations of the orientational ρ and phase δ structure of an ensemble of liquid amino acid crystals[13,14,18].

Figure 2 presents polarization images of the crystalline layers of the main types of amino acids of the human body.

We selected polycrystalline layers of three types of amino acids: glycine, methionine, and proline. This choice of objects for these compounds are the main "building" material for the formation of protein structures of biological structures.

Figures 3 to 8 show a series of experimentally measured Jones-matrix images of the real component of the "orientation" $R_{11}(m \times n)$ and "phase" $R_{12;21}(m \times n)$ elements and three-dimensional reconstructions of their values $N(R_{11})$, $N(R_{12;21})$, autocorrelation functions $G_{11}(\Delta x)$, $G_{12;21}(\Delta x)$ logarithmic spectral dependences $LgJ(G_{11})$; $LgJ(G_{12;21})$ of coordinate distributions of the values of the real component of the matrix elements of polycrystalline layers of the main types of glycine amino acids (Fig. 3 and Fig. 4), methionine (Fig. 5 and Fig. 6) and proline (Fig. 7 and Fig. 8), respectively[12].

The results of the study of the actual component of the Jones-matrix images of the elements of a set of polycrystalline layers of the main types of human amino acids showed:

1. The orientational structure of the directions of the optical axes of the network of partial crystals of amino acids has a significant effect. This is indicated by a wide range of changes ($0 \le R_{11} \le 1$) in the eigenvalues of the matrix element $R_{11}(m \times n)$ of the crystalline layers of the main types of amino acids (Fig. 3, Fig. 5, Fig. 7 Fragments (a)). Moreover, all the coordinate distributions of the real component of the “orientational” elements of the Jones matrix are individual for polycrystalline networks with different geometric constructions (Fig. 3, Fig. .5, Fig. 7. Fragments (b)).

2. The differences between the coordinate distributions of the real component of the "phase" $R_{12;21}$ element (Fig. 4, Fig. 6, Fig. 8, fragments (a)) of polycrystalline amino acid networks of different biochemical composition are not so expressive (Fig. 4, Fig. 6, Fig. 8 Fragments (b)) as for Jones-matrix images of "orientation" elements. Such a similarity, in our opinion, is associated with similar values of the birefringence index of the amino acids glycine, methionine, and proline.

3. The autocorrelation functions $G_{11;12;21}(\Delta x)$ of the coordinate distributions of the real component of the elements of the Jones matrix of crystalline amino acid layers with dendritic and spherolitic geometry are falling dependencies with pronounced fluctuations of eigenvalues (Fig. 3 and Fig. 5 fragments (c)).

4. The sets of values of the real component, "orientational" $R_{ik}(m \times n)$, of the elements of the Jones matrix $R_{12;21}(m \times n)$ are practically fractal; for the "phase" matrix element - multifractal. The corresponding logarithmic dependences $LgJ(G_{11})$ are characterized by a constant angle of inclination over the entire range of variation of the geometric

dimensions of partial crystals (Fig. 3, Fig. 5 and Fig. 7, fragments (d)). Dependencies $LgJ(G_{12;21})$ are characterized by broken approximating curves with two angles of inclination (Fig. 4, Fig. 6, and Fig. 8, fragments (d)). In our opinion, this fact can be associated with multiple scale and coordinate ordered changes in the orientation of the optical axes of partial crystals of amino acids with a simultaneous multiple change in the phase δ period.

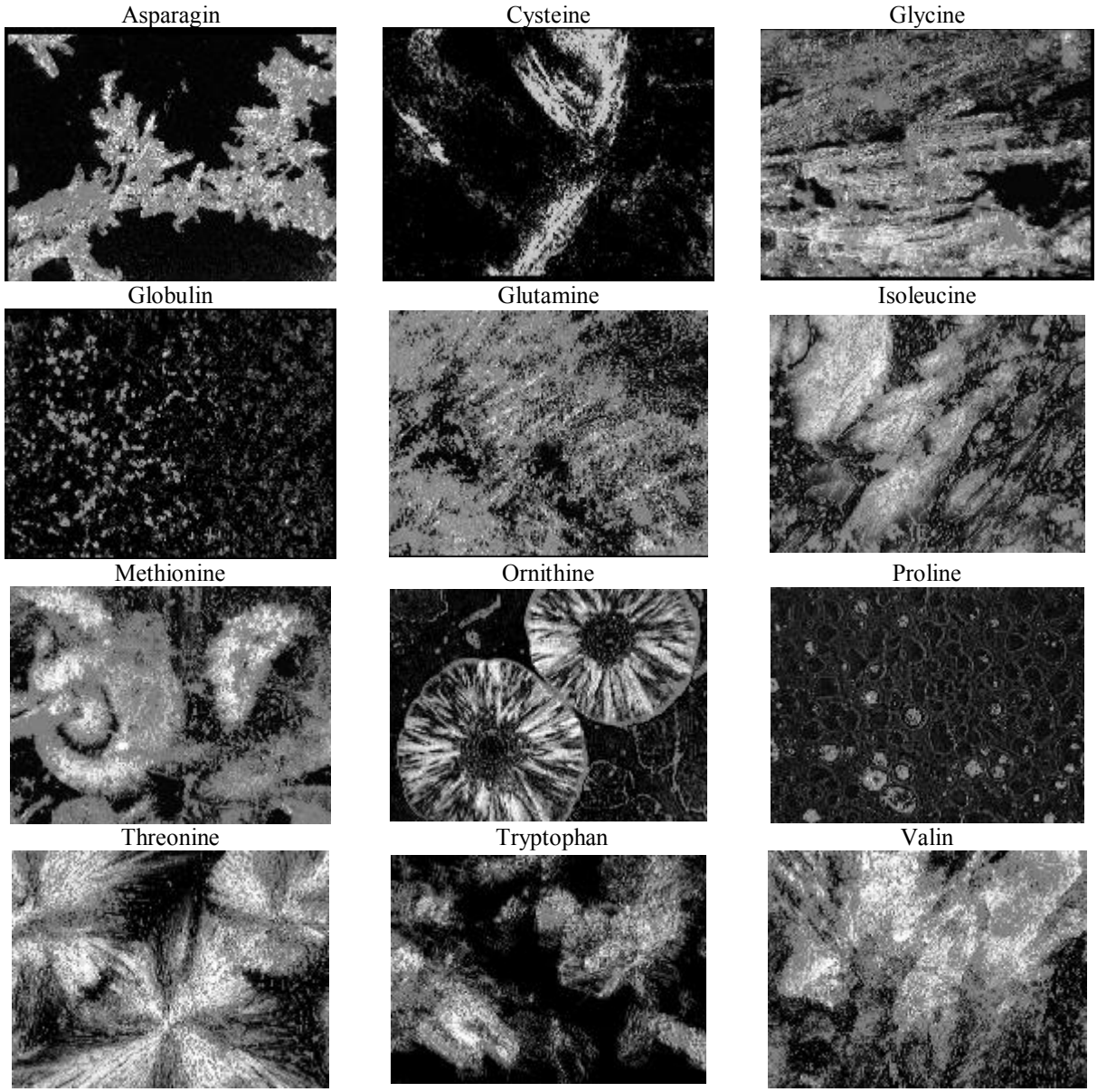

Figure 2. Polycrystalline networks of basic types of human amino acids

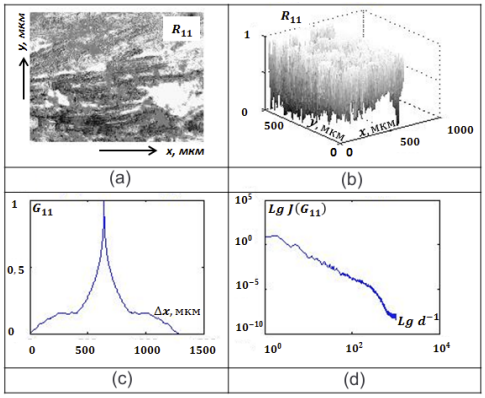

Figure 3. Coordinate (a), probabilistic (b), correlation (c) and self-similar (d) structure of the actual component of the element of the Jones matrix R_{11} of a polycrystalline network of a glycine layer

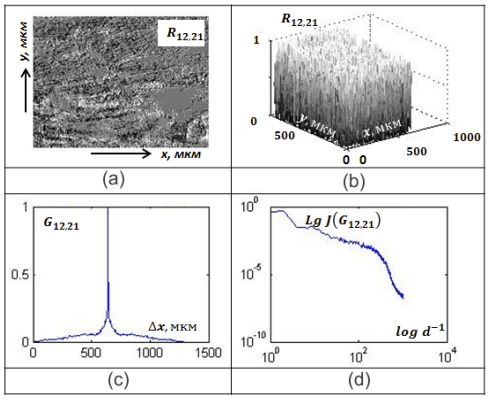

Figure 4. Coordinate (a), probabilistic (b), correlation (c) and self-similar (d) structure of the real component of the element of the Jones matrix $R_{12;21}$ of the polycrystalline network of the glycine layer

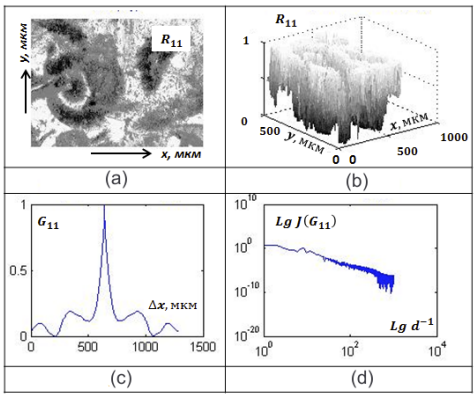

Figure 5. Coordinate (a), probabilistic (b), correlation (c) and self-similar (d) structure of the real component of the element of the Jones matrix R_{11} of the polycrystalline network of a mitionine layer

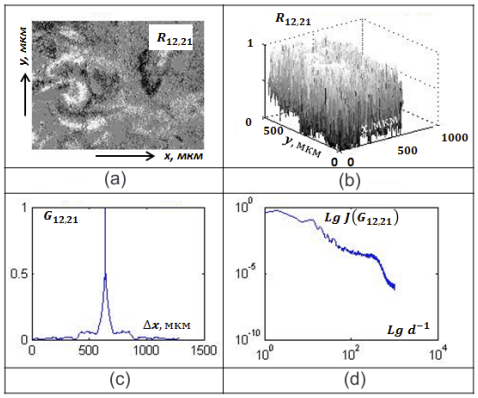

Figure 6. Coordinate (a), probabilistic (b), correlation (c) and self-similar (d) structure of the actual component of the element of the Jones matrix $R_{12;21}$ of the polycrystalline network of the mitionine layer

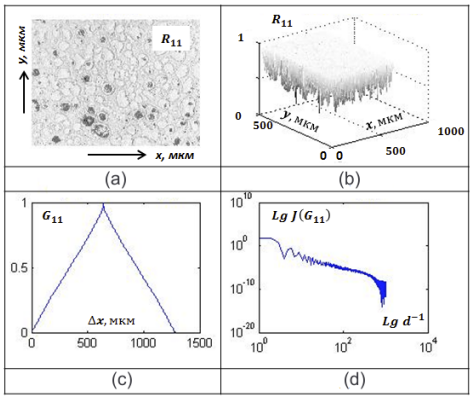

Figure 7. Coordinate (a), probabilistic (b), correlation (c) and self-similar (d) structure of the real component of the element of the Jones matrix R_{11} of a polycrystalline network of a proline layer

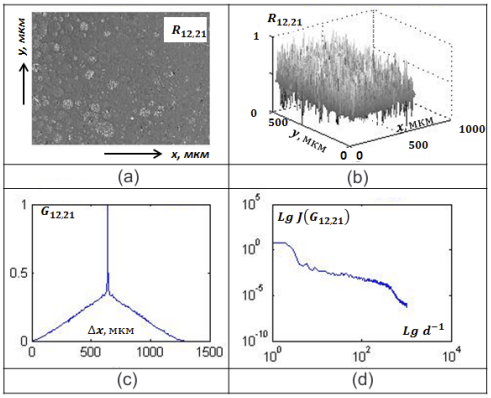

Figure 8. Coordinate (a), probabilistic (b), correlation (c) and self-similar (d) structure of the real component of the element of the Jones matrix $R_{12;21}$ of a polycrystalline network of a proline layer

The results of the quantitative analysis of the values and ranges of statistical, correlation, and spectral moments characterizing the coordinate distributions $R_{ik}(m \times n)$ of the real component of the elements of the Jones matrix of polycrystalline layers of the main types of amino acids are shown in Table 1.

Table 1 Statistical (M, σ, A, E), correlation ($K_{i=1;2;3;4}$), spectral ($S_{i=1;2;3;4}$) parameters of Jones-matrix images $R_{ik}(m \times n)$ of polycrystalline amino acid layers

$R_{11}(m \times n)$						$R_{12;21}(m \times n)$					
Glycine											
M	0.41	K_1	0.44	S_1	0.56	M	0.46	K_1	0.48	S_1	0.53
σ	0.21	K_2	0.14	S_2	0.19	σ	0.19	K_2	0.14	S_2	0.14
A	0.86	K_3	1.31	S_3	0.62	A	0.24	K_3	0.29	S_3	0.43
E	0.63	K_4	3.16	S_4	0.83	E	0.17	K_4	1.19	S_4	0.37
Methionine											
M	0.31	K_1	0.52	S_1	0.48	M	0.51	K_1	0.51	S_1	0.5
σ	0.15	K_2	0.11	S_2	0.13	σ	0.24	K_2	0.11	S_2	0.11
A	0.53	K_3	0.57	S_3	0.47	A	0.18	K_3	0.24	S_3	0.31
E	0.68	K_4	2.12	S_4	0.39	E	0.12	K_4	0.91	S_4	0.27
Proline											
M	0,39	K_1	0,45	S_1	0,56	M	0,48	K_1	0,48	S_1	0,52
σ	0,28	K_2	0,1	S_2	0,13	σ	0,32	K_2	0,07	S_2	0,09
A	0,12	K_3	0,24	S_3	0,48	A	0,12	K_3	0,36	S_3	0,21
E	0,09	K_4	1,38	S_4	0,27	E	0,09	K_4	1,15	S_4	0,18

4. CONCLUSIONS

Data on a laser micropolarimeter and its optical arrangement are given, in which the coordinate distributions of the real and imaginary component of the elements of the Jones matrix of optically thin polycrystalline layers are determined. The experimental results of the study of statistical, correlation and fractal parameters characterizing the actual components of the Jones-matrix images of polycrystalline networks of basic types of human amino acids are presented. Analysis of the results revealed that:

• The entire set of 1st, 4th order statistical, correlation, and spectral moments, which characterize the coordinate distributions of the real component of the elements of the Jones matrix, has individual sets of values that depend on the optical-geometric parameters of polycrystalline networks of amino acids.

• There is a satisfactory correlation between the data of computer simulation and the experimental study of the structure of the real component of Jones-matrix images.

• The disordering of the directions of the optical axes of partial crystals of amino acids is manifested in such changes in quantitative parameters: a decrease in the magnitudes of the statistical moments of the 3rd and 4th orders of the coordinate distribution of the real component of the “orientation” element of the Jones matrix according to the following geometry of polycrystalline networks "; Attenuation of oscillations of the autocorrelation functions of Jones-matrix images, as well as a decrease in the corresponding values th asymmetry ( ) and kurtosis ( ) of such dependences, the growth of the 3rd and 4th order spectral moments, which characterize the logarithmic dependences of the power spectra of the coordinate distribution of the real component of the "orientational" element of the Jones matrix.

The range of differences between the values of statistical, correlation and spectral moments of the 1st - 4th orders characterizing the distribution of the values of the real component of the "phase" elements of the Jones matrix of polycrystalline amino acid networks of various types times less than in the case of similar quantitative parameters for "orientational" Jones-matrix images.

REFERENCES

[1] Prysyazhnyuk, V. P., Ushenko, Yu. A., Dubolazov, A. V., Ushenko, A.G., and Ushenko, V.A., "Polarization-dependent laser autofluorescence of the polycrystalline networks of blood plasma films in the task of liver pathology differentiation," Applied Optics 55(12), B126-B132 (2016).

[2] Rovira, R. H., Tuzhanskyy, S. E., Pavlov, S. V., et al., "Polarimetric characterisation of histological section of skin with pathological changes," Proc. SPIE 10031, 100313E (2016).

[3] Rovira, R. H., Pavlov, S. V., Kaminski, O. S. and Bayas, M. M., "Methods of Processing Video Polarimetry Information Based on Least-Squares and Fourier Analysis," Middle-East Journal of Scientific Research, 16(9), 1201-1204 (2013).

[4] Timchenko, L. I., Pavlov, S. V., Kokryatskaya, N. I., et al., "Bio-inspired approach to multistage image processing," Proceedings of SPIE 10445, 104453M (2017).

[5] Wójcik, W, Cąkała, S., Kotyra, A., et al. "Analysis of the operation of an electrooptical Pockels effect", Proceedings of SPIE 3189, 110-121 (1997).

[6] Maciejewski, M., Surtel, W., Wójcik, W., et al., "Telemedical systems for home monitoring of patients with chronic conditions in rural environment," Annals of Agricultural and Environmental Medicine 21(1), 167-173 (2014).

[7] Ushenko, V. O., "Spatial-frequency polarization phasometry of biological polycrystalline networks," Optical Memory and Neural Networks (Information Optics) 22(1), 56-64 (2013).

[8] Angelsky, P. O., Ushenko, A. G., Dubolazov, A. V., Sidor, M. I., Bodnar, G. B., Koval, G. and Trifonyuk, L., "The singular approach for processing polarization-inhomogeneous laser images of blood plasma layers," Journal of Optics 15(4), 044030 (2013).

[9] Ushenko, O. G., Dubolazov, A. V., Balanets'ka, V. O., Karachevtsev, A. V. and Sydor, M., "Wavelet analysis for polarization inhomogeneous laser images of blood plasma," Proceedings of SPIE 8338, 83381H (2011).

[10] Wójcik, W., and Smolarz, A. (eds), [Information Technology in Medical Diagnostics], Taylor&Francis, London, 12-210 (2017).

[11] Pavlov, S. V., Kozhemiako, V. P., Kolesnik, P. F., et al., [Physical principles of biomedical optics], VNTU, Vinnytsya, 15-152 (2010).

[12] Pavlov, S. V., Tuzhanskyy, S. E., Kozlovska, T. I. and Kozak, A. V., "A simulation model of distribution of optical radiation in biological tissues, Visnyk VNTU 3, 191-195 (2011).

[13] Kholin, V. V., Chepurna, O. M., Pavlov, S. V., et al., "Methods and fiber optics spectrometry system for control of photosensitizer in tissue during photodynamic therapy," Proc. SPIE 10031, 1003138 (2016).

[14] Rovira, R. H., Tuzhanskyy, S. E., Pavlov, S. V., et al., "Polarimetric characterisation of histological section of skin with pathological changes," Proc. SPIE 10031, 100313E (2016).

[15] Dzierżak, R., "Comparison of the influence of standardization and normalization of data on the effectiveness of spongy tissue texture classification," Informatyka, Automatyka, Pomiary w Gospodarce i Ochronie Środowiska 9(2), 66-69 (2019).